LIMNOLOGY
and
OCEANOGRAPHY: METHODS

ASLO

Limnol. Oceanogr.: Methods 13, 2015, 288–302

doi: 10.1002/lom3.10025

Tracing carbon fixation in phytoplankton—compound specific and total ^{13}C incorporation rates

Julia Grosse,*[1] Peter van Breugel,[2] Henricus T. S. Boschker[1]
[1]Department of Marine Microbiology, NIOZ Royal Netherlands Institute for Sea Research, Yerseke, The Netherlands
[2]Analytical Laboratory, NIOZ Royal Netherlands Institute for Sea Research, Yerseke, The Netherlands

Abstract

Measurement of total primary production using ^{13}C incorporation is a widely established tool. However, these bulk measurements lack information about the fate of fixed carbon: the production of major cellular compounds (carbohydrates, amino acids, fatty acids, and DNA/RNA) is affected by for instance nutrient availability as their C:N:P requirements differ. Here, we describe an approach to combine established methods in gas chromatography/isotope ratio mass spectrometry (GC/C-IRMS) and recently developed methods in liquid chromatography/IRMS (LC/IRMS) to trace stable isotope incorporation into neutral carbohydrates, amino acids, and fatty acids, and compare their production to total carbon fixation rates. We conducted a trial study at stations in the North Sea where different nutrients were limiting. There was variation in the fate of fixed carbon at these sites. The majority of fixed carbon (64–71%) was incorporated into neutral carbohydrates, followed by amino acids (19–32%) and fatty acids (4–9%). The sum of carbon fixation into these three fractions accounted for 81–116% of total carbon fixation. P- and N-limitation increased the biosynthesis of storage lipids and storage carbohydrates while N-limitation decreased synthesis of amino acid proline with a concurrent increase in glutamic acid + glutamine. This new approach provides the capability to determine direct effects of resource limitation and the consequences for the physiological state of a phytoplankton community. It may thereby enable us to evaluate the overall quality of phytoplankton as a food source for higher trophic levels or trace consumption of phytoplankton through the food web.

Approximately half of the global net primary production is performed in the ocean (Field et al. 1998) and phytoplankton forms the basis of most food webs in the sea. Methods to estimate primary production have been around for decades and remote sensing as well as several experimental approaches are currently in use (Cullen 2001). Widely used methods for determining rates of primary production in the field are based on the incorporation of carbon isotopes, both radioactive (^{14}C) and stable (^{13}C), into phytoplankton biomass (Steeman-Nielsen 1952; Montoya et al. 1996). A wealth of data is available on primary production rates in different areas (Gosselin et al. 1997; Carpenter et al. 2004; Shiozaki et al. 2010), over different time scales (Karl et al. 1996; Gallon et al. 2002) and from culture studies (Degerholm et al. 2006; Wannicke et al. 2009), providing a valuable tool to estimate total productivity of a system. However, total primary production rates do not give any information on the intracellular fate of the fixed carbon and, therefore, the nutritional value of it to higher trophic levels. It is well known that carbon uptake and consequently phytoplankton growth are regulated by many factors such as light or nutrient availability. Phytoplankton stressed by too much light or too little nutrient availability react by storing carbon in the form of storage carbohydrates and/or triglycerides (Granum et al. 2002; Borsheim et al. 2005). Both of those compounds are carbon rich but do not contain nitrogen (N) or phosphorus (P), causing a shift in phytoplankton C:N:P ratios and a decline in the nutritional value of phytoplankton to consumers (Sterner et al. 1993; Plath and Boersma 2001).

The diversity in nutrient N:P ratios faced by marine phytoplankton led to the development of models to predict changes in the growth strategy of phytoplankton (Klausmeier et al. 2004). Low cellular N:P ratios would be present in phytoplankton adapted to high growth rates, which have the resources to invest in growth machinery high in both N and P (e.g., ribosomal RNA [rRNA]) (Falkowski 2000). In contrast, to sustain growth under low resource availability, phytoplankton invests in resource acquisition machinery (pigments and proteins), which is rich in N but mostly lacks P, resulting in high N:P ratios (Geider and LaRoche 2002). Confirming those strategies in natural phytoplankton communities and changes between them caused by changes in

*Correspondence: julia.grosse@nioz.nl

resource availability is challenging and investigations on the level of individual compounds have been rare until a few years ago and are mainly based on changes in compound concentrations following the addition or reduction of nutrients (Granum et al. 2002; Mock and Kroon 2002). Detection of significant changes in the compound concentrations requires long-term incubations (several days to weeks), which can simultaneously cause undesired changes in the phytoplankton community and may not lead to field relevant results (Beardall et al. 2001). Charpin et al. (1998) and Suárez and Marañón (2003) used the incorporation of ^{14}C to quantify carbon allocation into different macromolecule groups (total lipids, proteins, and polysaccharides), but due to for instance special regulations of handling radioactive material, this method is not widely applied.

In recent years, the advances in compound specific stable isotope analysis (CSIA) by either gas chromatography (GC) or liquid chromatography (LC) in combination with isotope ratio mass spectrometry (IRMS) have made it possible to obtain specific isotope information of a wide range of compounds directly from complex mixtures. This opens possibilities to use ^{13}C stable isotopes in the same way as they are already used for total primary production measurements (bulk) but to study phytoplankton communities on a more detailed compound specific level by following the photosynthetically fixed carbon into macromolecules such as individual fatty acids, amino acids, and carbohydrates.

Many studies are already available on the incorporation of carbon into a particular fraction of fatty acids, the phospholipid derived fatty acids (PLFA), to determine the activity or composition of specific groups of phytoplankton or bacteria (Middelburg et al. 2000; Van Den Meersche et al. 2004; Dijkman et al. 2010). Separation of individual fatty acids is performed on a GC and, therefore, fatty acids have to be derivatized. As only one extra carbon has to be added per fatty acid, it makes corrections for natural abundance $\delta^{13}C$ values straightforward. However, requirements of heavy derivatization of carbohydrates and amino acids for separation on a GC make determination of $\delta^{13}C$ natural abundance studies prone to errors (Rieley 1994) and require extensive corrections. Therefore, the GC/C-IRMS method is commonly used for tracer studies with ^{13}C and ^{15}N incorporation into amino acids (Veuger et al. 2007; Oakes et al. 2010) as well as food web studies using natural abundance of ^{15}N in amino acids (McCarthy et al. 2013). The recently developed LC/IRMS methods make the derivatization of carbohydrates and amino acids unnecessary and are being introduced to a wide range of fields including geochemistry, nutrition, paleodiet, ecology, forensics, and medicine (Godin et al. 2007). Currently, the majority of studies focus on the natural abundance of ^{13}C in those compounds, usually used to identify sources and only a limited number of publications included ^{13}C amended tracers to investigate carbon incorporation into different compounds (McCullagh et al. 2008; Oakes et al. 2010; Miyatake et al. 2014). In all cases, carbon incorporation was mainly determined for one macromolecule group, for example, amino acids or PLFAs, and information is lacking on how carbon is simultaneously distributed between different pools of macromolecules. Combining these methods to determine fatty acid, amino acid, and neutral carbohydrate synthesis by ^{13}C labeling would give insight into the biochemical fate of fixed carbon and the physiological state of the phytoplankton community in terms of resource limitation.

In this study, we show how a combination of established GC/C-IRMS and recently developed LC/IRMS methods (Fig. 1) can be used to identify the composition and biosynthesis of individual fatty acids, amino acids, and carbohydrate pools of natural phytoplankton communities. We modified existing protocols to make them applicable to marine phytoplankton and added clean up steps to reduce interference from impurities in the LC-methods. By combining the GC and LC approaches with ^{13}C measurements on an IRMS, the biosynthesis rates of these individual compounds can be calculated. Overall, these three major macromolecule groups can be examined in detail and be compared with bulk measurements of primary production. This makes it possible to provide an overview of the ability of phytoplankton to allocate carbon fixed through photosynthesis into different functional groups of macromolecules and to study how phytoplankton copes with differences in resource availability.

Materials and procedures

Field experiment

For the trial experiment, we chose three sites in the North Sea (Fig. 2) with different physical and chemical features. The Coastal Station is only four kilometers offshore with a water depth of eight meters and, therefore, heavily influenced by runoff from land, mainly through nutrient-rich discharge from the river Rhine. The Oyster Ground is a relatively deep station (46 m) and stratified during summer. The Dogger Bank station is shallower (28 m) and complete mixing of the water column is possible year around.

Labeling of phytoplankton with ^{13}C-bicarbonate

A labeling experiment with stable isotope tracer ^{13}C-labeled bicarbonate was performed during a North Sea cruise on board the R/V Pelagia in May 2012. For the experiments, subsurface water (seven meters) was obtained with Niskin bottles, transferred to 10 L carboys and enriched with ^{13}C-sodium bicarbonate (99% ^{13}C). The final labeling concentration reached 1.5–2% ^{13}C of the ambient dissolved inorganic carbon (DIC) concentration. To determine the absolute ^{13}C enrichment in DIC, 10 mL of sample were sealed in a crimp vial without gas bubbles, a 2 mL helium headspace was created, and after acidification the headspace was analyzed for CO_2 concentration and ^{13}C-content by a Flash EA 1112 Series elemental analyzer (EA) coupled via a Conflo III

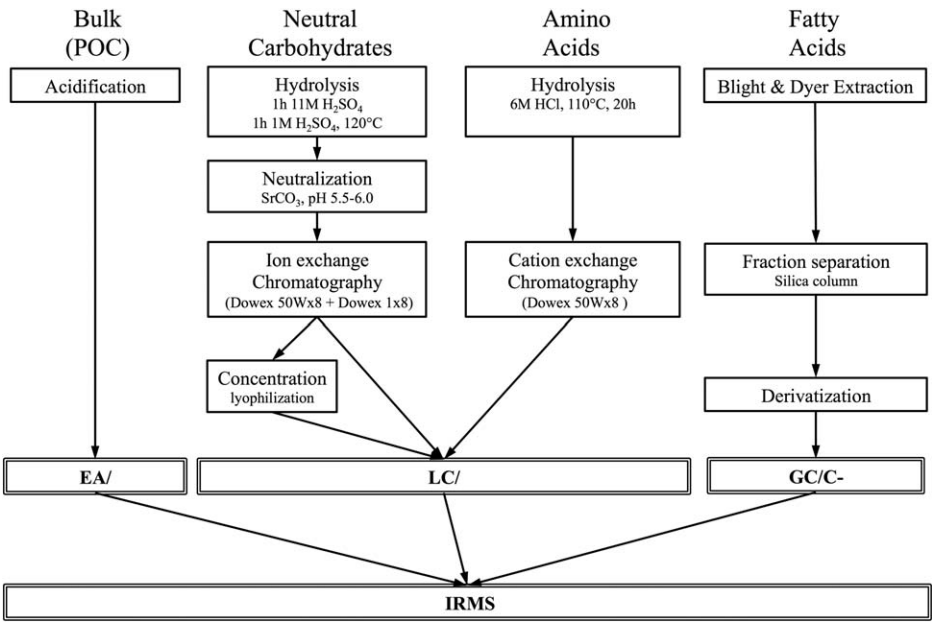

Fig. 1. Flow chart with overview of methods used in the approach of ^{13}C tracing into the macromolecules.

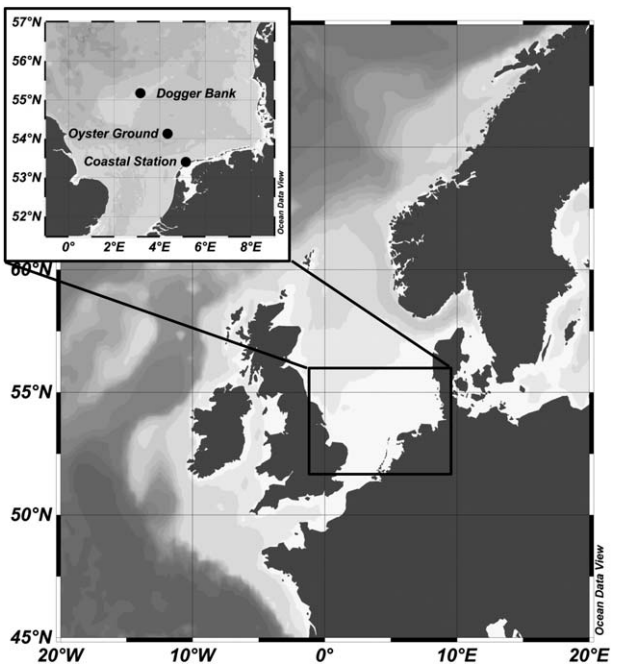

Fig. 2. Map of the sampling area in the North Sea.

interface to a Delta V advantage IRMS (all from Thermo Fisher Scientific, Bremen, Germany) (Moodley et al. 2005). To keep light and temperature close to in situ conditions, the carboys were white and reduced ambient light levels by approximately 50%. They were incubated in flow-through incubators on deck, which assured stable temperatures. The incubations lasted for 24 h before the experiment was terminated by splitting the carboy content into five equal volumes, which were filtered over precombusted GF/F filters (Whatman, 47 mm ∅, 0.45 μm pore-size, 4 h at 450°C). Aliquot samples were taken for particulate organic carbon (POC), fatty acid, amino acid, and neutral carbohydrate analysis as well as an additional filter, which served as a backup. A volume between 1.0 L and 2.0 L was filtered per aliquot, depending on the phytoplankton density. All filters were stored frozen at −80°C until analysis (POC) or extraction of the macromolecules. All incubations were performed in duplicate and initial, unlabeled samples for POC and all macromolecule groups were taken at the beginning of each of the incubations.

Chlorophyll *a* and nutrient concentrations

Samples for chlorophyll *a* (Chl *a*) and other pigments were collected on GF/F filters (Whatman, 47 mm ∅, 0.45 μm pore-size) and stored at −80°C until analysis. Pigments were extracted with 10 mL of 90% acetone using a CO_2—gas cooled bead-beater followed by centrifugation (3 min, 1500 rpm) and the supernatant was injected onto a C18-reverse-phase column (Allsphere^{TM} ODS-2, Thermo Fisher Scientific). Gradient mixing pumps delivered three mobile phase solvents: (1) methanol/ammonium acetate, (2) 90% acetonitrile, and (3) 100% ethyl acetate (Rijstenbil 2003 and references therein). Pigments were identified and quantified using commercially available standards (Dijkman and Kromkamp 2006).

Dissolved nutrient samples were taken by filtering water through a 0.2 μm Acrodisc filter (Pall Netherlands, Mijdrecht, The Netherlands). The concentrations for ammonium (NH_4^+), nitrate (NO_3^-), nitrite (NO_2^-), phosphate

(PO_4^{3-}), and silicate ($Si(OH)_4$) were analyzed using a QuAAtro autoanalyzer (SEAL Analytical) according to the manufacturers instruction.

Total particulate organic carbon

Before analysis, frozen filters were lyophilized overnight, and a section of the filter (1/4 or less, depending on the amount of material on the filter) was acidified over fuming HCl to remove inorganic carbon, and subsequently packed into tin cups. The analysis was performed on a Flash EA 1112 Series EA coupled via a Conflo III interface to a Delta V advantage IRMS (all from Thermo Fisher Scientific) to obtain organic carbon content and $\delta^{13}C$ values.

Liquid chromatography/isotope ratio mass spectrometry

As samples have to be introduced to the IRMS instrument in a gaseous form, GC/C-IRMS remained the only method of choice for a long time to separate compounds for isotopic analysis. However, sample preparation is extensive and after extraction most compounds have to be derivatized.

Connecting LC to IRMS was challenging because separation is achieved within a liquid eluent. However, after the introduction of the LC Isolink interface (Thermo Fisher Scientific), which uses a wet-oxidation process to convert separated compounds on-line to CO_2 (Krummen et al. 2004), LC/IRMS became a viable alternative to GC/C-IRMS for the analysis of many biological compounds. After LC separation, the organic compound is mixed with acid (phosphoric acid) and an oxidant (sodium peroxydisulfate), heated in a reactor to 99.9°C and thereby converted into CO_2. The CO_2 gas subsequently crosses the membrane separation unit into a helium flow and is introduced into the IRMS instrument. Constraints of this method mainly arise in the choice of eluents and analytical columns. To keep the CO_2 background low, only water-based inorganic solutions and buffers can be used as eluents and analytical columns should have low bleeding characteristics. However, amino acids and carbohydrates can be analyzed without prior derivatization and subsequent corrections of $\delta^{13}C$ values are not necessary (McCullagh et al. 2006; Boschker et al. 2008). The precision of the LC/IRMS is comparable to that of other continuous flow techniques and better than those reported for the GC/C-IRMS remaining below 0.4‰ for individual compounds even at low compound concentrations (detection limit varies by compound, ranging between 36 ng C and 150 ng C, McCullagh et al. 2006; Boschker et al. 2008).

Neutral carbohydrate extraction and analysis

Neutral carbohydrates were extracted using a modified version of the protocol described by Boschker et al. (2008). In detail, filters were cut into small pieces, and 1 mL 11 mol L^{-1} H_2SO_4 was added to wet the entire filter. The samples were left at room temperature for 1 h before the H_2SO_4 was diluted with MilliQ to a final concentration of 1.1 mol L^{-1}, followed by a hydrolysis at 120°C for 1 h. After cooling the samples rapidly on ice, they were neutralized to a pH of 5.5–6.0 by adding $SrCO_3$. The $SrSO_4$ was removed by centrifugation and the supernatant was frozen overnight to further precipitate any remaining $SrSO_4$. After a subsequent slow thawing of samples at 4°C, we added a clean-up step as described by Boschker et al. (1995), to remove substances that interfered with the LC/IRMS analysis. The samples were run over a double bed resin containing equal amounts of cation exchange resin (2 mL of Dowex 50Wx8, hydrogen form, Sigma-Aldrich) and anion exchange resin (2 mL of Dowex 1x8, Sigma-Aldrich, purchased in chlorine form, used in carbonate form, see below) to remove inorganic and organic salts. The cation exchange resin was activated by subsequent washing with MilliQ, 2 mol L^{-1} NaOH, 2 mol L^{-1} HCl, and MilliQ and was used to trap impurities such as amino acids, which can interfere with the signal from neutral carbohydrates. The anion exchange resin was transformed from a chlorine form into a carbonate form by washing with MilliQ, 0.1 mol L^{-1} Na_2CO_3, and MilliQ before use (Abaye et al. 2011). The samples were run over the mixed-resin bed column and collected in glass vials. Unconcentrated samples can be filtered (0.2 μm PVDF filters) and analyzed directly by LC/IRMS as long as the dilution from MilliQ in the resin slurry is accounted for. However, in our field samples neutral carbohydrate concentrations were so low that the samples needed to be concentrated before measurement. Therefore, the samples were frozen again, lyophilized to complete dryness, subsequently redissolved in 1 mL MilliQ and filtered (0.2 μm PVDF filters) before analysis.

Neutral carbohydrate concentrations and $\delta^{13}C$ values were measured on a LC/IRMS system, equipped with a Surveyor system consisting of a high performance liquid chromatography pump (MS Pump Plus) and an Autosampler Plus autoinjector and coupled to an Delta V advantage IRMS instrument via a LC Isolink interface (all Thermo Fisher Scientific). Isodat software 3.0 (Thermo Fisher Scientific) was used to control the LC/IRMS system and for data collection. Separation of neutral carbohydrates was performed using an Aminex HPX-87H column (300 × 7.8 mm, 9 μm particle size; Bio-Rad) with 0.02% 12 mol L^{-1} H_2SO_4 as mobile phase at a flow rate of 0.4 mL min^{-1} and the column was kept at a temperature of 22°C. The run time was 50 min and a 50 μL sample loop was used for injection. The injected sample volumes ranged from 10 μL (partial loop injection) to 50 μL (full loop injection), depending on neutral carbohydrate concentrations. To obtain 50 ng of C per compound, we suggest that an amount > 70 μg POC should be extracted for neutral carbohydrates when using the Aminex HPX-87H column.

Commercially available neutral carbohydrates (Sigma-Aldrich) were dissolved in MilliQ water and injected individually to identify elution order. The Aminex HPX-87H column baseline separates glucose (Glu) from all other carbohydrates, while galactose (Gal), xylose (Xyl), mannose

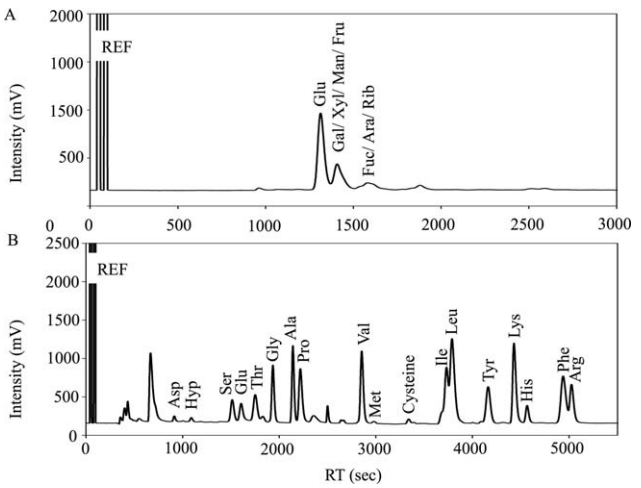

Fig. 3. Example chromatographs for compound specific analysis of carbohydrates (A) and amino acids (B) at the Coastal Station. Carbohydrates shown are: glucose (Glu), co-elution of galactose/xylose/mannose/fructose (Gal/Xyl/Man/Fru) and co-elution of fucose/arabinose/ribose (Fuc/Ara/Rib). Eighteen amino acids are shown: aspartic acid + asparagine (Asp), hydroxiproline (Hyp), serine (Ser), glutamic acid + glutamine (Glu), threonine (Thr), glycine (Gly), alanine (Ala), proline (Pro), valine (Val), methionine (Met), cysteine, isoleucine (Ile), leucine (Leu), tyrosine (Tyr), lysine (Lys), histidine (His), phenylalanine (Phe), and arginine (Arg). REF, reference pulse; RT, retention time.

(Man), and fructose (Fru) co-elute in a second peak. A third peak contains fucose (Fuc), arabinose (Ara), and ribose (Rib; Fig. 3A, example from an environmental sample). Alternatively, the Carbopac PA20 column (Thermo Fisher Scientific) can be used according to Boschker et al. (2008), which is capable of separating all eight carbohydrates. However, in our case the required injection volume was up to 200 μL to achieve proper detection. At these high quantities, we encountered interference with the column (see Discussion), and therefore, suggest collecting higher amounts of POC (> 240 μg) when using the Carbopac PA20 column. A mixture of aforementioned external standards was used to calculate carbohydrate concentrations using a calibration line and to monitor LC/IRMS performance. The $\delta^{13}C$ values of powdered external standards analyzed by EA/IRMS were in excellent agreement with values determined by LC/IRMS using the Aminex HPX-87H column and values reported by Boschker et al. (2008). International glucose references IAEA-309A and IAEA-309B, both enriched in ^{13}C, were also analyzed to determine accuracy of LC/IRMS. Measured $\delta^{13}C$ values were within the standard deviation of certified values.

Amino acid extraction and analysis

To obtain hydrolyzable amino acids, we applied a modified version of the protocol from Veuger et al. (2005), which describes the extraction of amino acid for analysis by GC/C-IRMS. In detail, GF/F filters were cut into small pieces and hydrolyzed in 2 mL 6 mol L^{-1} HCl at 110°C for 20 h. There was no need to apply an acid-washing step, as in the original protocol, as the amount of inorganic carbon on the filter was much lower than in sediment samples. After cooling, the samples were diluted to a final concentration of 1 mol L^{-1} HCl by adding 10 mL MilliQ. The samples were subjected to cation exchange chromatography with Dowex 50Wx8 resin (hydrogen form, Sigma-Aldrich), which was activated as described above, filled into glass columns and prerinsed with 10 mL of MilliQ. Samples were added to the column, and washed with 20 mL MilliQ to remove salt and organic compounds. Amino acids were eluted from the column with 12 mL of 2 mol L^{-1} NH_4OH, collected in glass beakers and dried overnight on a heating plate ($\sim$ 60°C). Once dry, samples were redissolved in 1 mL of MilliQ, filtered (0.2 μm PVDF filters) and measured on the same LC/IRMS as described above. Separation of amino acids was performed using a Primsep A column (250 $\times$ 3.2 mm, 5 μm particle size; SIELC) with a modified linear gradient program according to McCullagh et al. (2006). Mobile phase A (100% degassed MilliQ water) was used for the first 22 min, followed by a linear gradient to 100% mobile phase B (0.2% 12 mol L^{-1} H_2SO_4) from 22 min to 75 min, and afterward 100% mobile phase B until the end of the run (115 min). A subsequent column flushing of 10 min with mobile phase A reconditioned the column for the next sample injection. The flow rate was constant at 0.5 mL min^{-1} and a 50 μl sample loop was used for injection with sample volumes ranging from 10 μL to 50 μL, depending on amino acid concentrations. To obtain 50 ng of C per compound, we suggest that a minimum amount of 200 μg POC should be extracted for amino acids.

Amino acids were identified by individually injected standards of commercially available amino acids (Sigma-Aldrich, Fig. 3B, example from an environmental sample). Amino acid concentrations were calculated using a calibration line of a mixture of aforementioned external standards, which was also used to monitor LC/IRMS performance.

Fatty acids extraction and analysis

The extraction was performed according to Boschker (2004). In short, the total lipid extract was obtained following the protocol of Bligh and Dyer (1959), and subsequently separated into storage lipids, glycolipids, and phospholipids by silicate column chromatography with 7 mL chloroform, 7 mL acetone, and 15 mL methanol. However, Boschker (2004) only focus on the recovery of the phospholipid fraction contained in the methanol and totally discards the other two fractions. In this approach, we also collect the storage lipid fraction in the chloroform and the glycolipid fraction in the acetone. All three fractions were dried down and derivatized to fatty acid methyl esters (FAMEs) using mild alkaline methanolysis (1 mL 0.2 mol L^{-1} sodium methylate, 15 min at 37°C) followed by a hexane extraction. This resulted in the three FAME solutions containing (1) storage

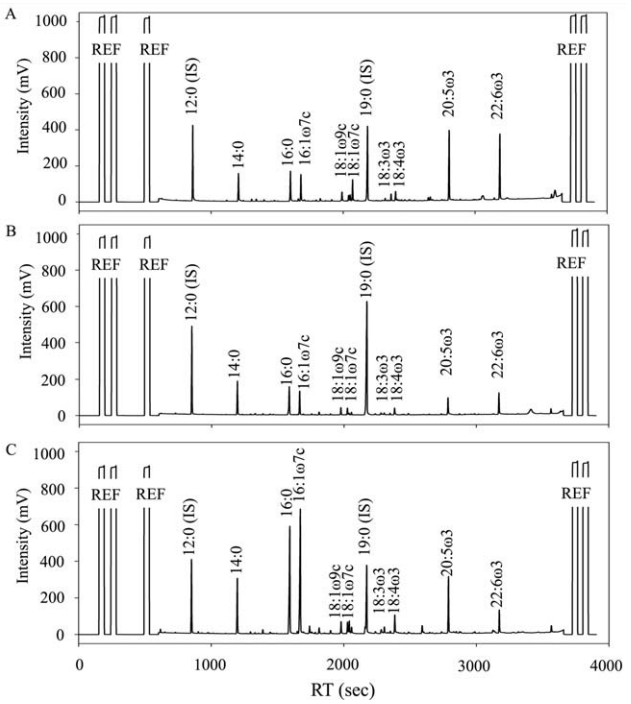

Fig. 4. Examples of chromatographs for analysis of different fatty acid fractions—methanol (A), acetone (B), chloroform (C) at the Coastal Station. All samples originate from the same total lipid extract. It should be noted that the amounts of IS 12:0 and 19:0 (saturated fatty acid methyl ester with chain-lengths of 12 and 19 carbon atoms) added to samples were the same in all three fractions. Due to different amounts of fatty acids within different fractions the injection volume was adapted, which resulted in different peak heights of 12:0 and 19:0 in the different chromatograms. REF, reference pulse; RT, retention time.

lipid derived fatty acids (SLFAs), (2) glycolipid derived fatty acids (GLFAs), and (3) PLFAs. The FAMEs 12:0 and 19:0 were added as internal standards (IS). Concentrations and $\delta^{13}C$ of individual FAMEs were measured by GC/C-IRMS (controlled by Isodat 2.0 software); a HP G1530 GC (Hewlet Packard/Agilent) was connected to a Delta-plus IRMS via a type III combustion interface (both from Thermo Fisher Science). For FAME separation, the very polar analytical column BPX-70 (50 m length, 0.32 mm diameter, 0.25 μm film; Scientific Glass Engineering) was used because it achieves better separation in polyunsaturated fatty acids (PUFAs) with 18 or more carbon atoms that are common in phytoplankton. An autosampler was used for injection of samples. Samples were injected at 36°C using a Cooled Injection System (Gerstel, Mülheim a.d.). After the hexane solvent was evaporated, the injector was heated up rapidly to 300°C; the split-less period was 1.5 min and the column flow was kept constant at 2 mL min^{-1}. The following temperature program was applied: initial 60°C for 2 min, then to 120°C with + 25°C min^{-1}, and hold for 5 min, then to 220°C with + 2°C min^{-1}, to 240°C with + 20°C min^{-1}, and hold 3 min resulting in a total runtime of 55 min.

Fatty acids contribution to total biomass can be small (< 5% of total POC) and, therefore, a substantial amount of biomass is required for extractions, especially if total fatty acids will be further separated into several fractions. We, therefore, suggest a minimum amount of 600 μg POC should be extracted for fatty acids.

For the identification of compounds, we calculated the relative retention time for each peak using the retention times of IS FAMEs 12:0 and 19:0 as well as naturally occurring 16:0 and compared them to a list of reference standards. The concentrations of the identified fatty acids were calculated based on the known amounts of the FAME 19:0 IS added to each sample. All three fractions were measured separately (Fig. 4A–C, examples from an environmental sample), evaluated separately and concentrations and biosynthesis rates for all fatty acids within one fraction were summed up at the end to obtain concentrations and biosynthesis rates for the respective fraction as well as the total fatty acid content. Fatty acids were notated A:BωC, where A is the number of carbon atoms in the fatty acid, B the number of double bonds, and C the position of the first double bond relative to the aliphatic end. An additional "c" indicates the *cis*-orientation of the double bond (e.g., 18:2ω6c).

Calculation of ^{13}C uptake rates

Carbon stable isotope ratios are expressed in the $\delta^{13}C$ notation:

$$\delta^{13}C_{sample}(‰) = \left(\left(R_{sample}/R_{VPDB}\right)-1\right)\times 1000,$$

where R_{sample} and R_{VPDB} denote the $^{13}C/^{12}C$ ratio in the sample and the international standard, Vienna Pee Dee Belemnite (for carbon $R_{VPDB} = 0.0111802 \pm 0.0000009$), respectively.

To quantify bulk carbon fixation and synthesis rates of the different compounds, the absolute amount of ^{13}C incorporated into different carbon pools above background was calculated. These values are expressed as excess ^{13}C (nmol $^{13}C\ L^{-1}$) and calculated in Eq. 1:

$$\text{Excess}^{13}C_{sample}\left[\left(\frac{(\delta^{13}C_{sample}/1000+1)\times R_{VPDB}}{(\delta^{13}C_{sample}/1000+1)\times R_{VPDB}+1}\right) - \left(\frac{(\delta^{13}C_{background}/1000+1)\times R_{VPDB}}{(\delta^{13}C_{background}/1000+1)\times R_{VPDB}+1}\right)\right]\times \text{concentration}_{sample}, \quad (1)$$

where $\delta^{13}C_{\ sample}$ refers to the $\delta^{13}C$ value of bulk material (POC) or the compound of interest at the end of the incubation, $\delta^{13}C_{background}$ denotes the $\delta^{13}C$ value of the unlabeled POC or compounds before the addition of ^{13}C-DIC, $\text{concentration}_{sample}$ denotes the concentration of POC or compound in nmol of carbon per liter (nmol C L^{-1}) at the end of the incubation.

To determine total carbon incorporation, the enrichment of the DIC pool with ^{13}C has to be calculated (Eq. 2).

Table 1. Overview of physical parameters, nutrients, nutrient ratios, and concentrations of particulate organic carbon (POC, averages ± SD [$n = 2$]).

	Coastal Station	Oyster Ground	Dogger Bank
Temperature (°C)	11.76	8.70	9.27
Salinity (PSU)	31.76	34.70	35.03
NO_3^- (μmol L^{-1})	7.51	0.63	0.02
NO_2^- (μmol L^{-1})	0.26	0.04	0.01
NH_4^+ (μmol L^{-1})	1.81	0.61	0.18
PO_4^{3-} (μmol L^{-1})	0.05	0.16	0.06
N: P (mol mol^{-1})	191.6	8.0	3.5
$Si(OH)_4$ (μmol L^{-1})	0.37	1.39	0.09
POC (μmol L^{-1})	44.17±1.26	12.72±1.58	17.83±1.06

Table 2. Pigment concentrations and ratios of selected pigments. Averages ± SD ($n = 2$), nd, not detected.

	Coastal Station	Oyster Ground	Dogger Bank
Alloxanthin (μg L^{-1})	nd	0.02±0.01	nd
Chl *a* (μg L^{-1})	3.08±0.03	0.42±0.04	0.77±0.03
Chl *b* (μg L^{-1})	0.01±0.00	0.08±0.00	0.02±0.00
Chl *c* 1 + 2 (μg L^{-1})	0.55±0.02	0.05±0.01	0.11±0.01
Diadinoxanthin (μg L^{-1})	0.16±0.03	0.02±0.01	0.12±0.01
Diatoxanthin (μg L^{-1})	0.02±0.01	nd	nd
Fucoxanthin (μg L^{-1})	1.89±0.05	0.12±0.02	0.34±0.03
Zeaxanthin (μg L^{-1})	nd	0.01±0.01	0.01±0.01
Chl *a*: Fucoxanthin	1.6±0.1	3.5±0.1	2.3±0.1
Chl *a*: Chl*c*	5.6±0.2	8.1±0.1	7.3±0.2

$$\text{Enrichment DIC} = \left(\frac{(\delta^{13}C_{\text{DICsample}}/1000+1)\times R_{\text{VPDB}}}{(\delta^{13}C_{\text{DICsample}}/1000+1)\times R_{\text{VPDB}}+1}\right) - \left(\frac{(\delta^{13}C_{\text{DICbackground}}/1000+1)\times R_{\text{VPDB}}}{(\delta^{13}C_{\text{DICbackground}}/1000+1)\times R_{\text{VPDB}}+1}\right) \quad (2)$$

where $\delta^{13}C_{\text{DICsample}}$ refers $\delta^{13}C$ of DIC in carboys at the end of the incubation and $\delta^{13}C_{\text{DICbackground}}$ denotes $\delta^{13}C$ of DIC before the addition of ^{13}C-DIC.

Biosynthesis rates (nmol C (μmol POC)$^{-1}$ d^{-1}) are calculated as followed:

$$\text{Biosynthesis rate} = \left[\left(\frac{\text{Excess } ^{13}C_{\text{sample}}}{\text{Enrichment DIC}}\right)\right] / \text{POC}_{\text{concentration}}/\Delta t\times 24 \quad (3)$$

where, $\text{POC}_{\text{concentration}}$ is the concentration of POC (μmol L^{-1}) at the end of the incubation and Δt is the incubation time in hours. A multiplication with 24 gives daily rates. Rates normalized to biomass allow comparison between different phytoplankton communities over spatial or temporal scales.

Concentrations and biosynthesis rates were calculated for each individual compound per duplicate. Concentrations and biosynthesis rates of subgroups (e.g., SLFA, GLFA, PLFA) or total macromolecule groups (total fatty acids, amino acids, and carbohydrates) were obtained by summing all individual biosynthesis rates within that group per duplicate. Afterward averages and standard deviations were calculated ($n = 2$).

Assessment

Station characterization

The nutrient availability differed at the three North Sea stations during the trial experiment in May 2012 (Table 1). Dissolved inorganic nitrogen concentration ($NO_3^- + NO_2^- + NH_4^+$) declined from 9.6 μmol L^{-1} to 1.3 μmol L^{-1} to 0.2 μmol L^{-1} at the Coastal Station, the Oyster Ground, and the Dogger Bank, respectively. Phosphate concentrations increased from 0.05 μmol L^{-1} to 0.16 μmol L^{-1} and went back down to 0.06 μmol L^{-1} at the Coastal Station, the Oyster Ground, and the Dogger Bank, respectively. This led to N:P nutrient ratios of 192 at the Coastal Station, 8 at the Oyster Ground, and 3.5 at the Dogger Bank. Assuming Redfield ratio (N:P 16: 1), this would characterize the Coastal Station as P-limited while the Oyster Ground and Dogger Bank were N-limited. Furthermore, the dominant nitrogen source at the Dogger Bank was NH_4^+, which suggests it was a regenerative system. Silicate ($Si(OH)_4$) concentrations were below 2 μmol L^{-1} at all stations, a threshold for allowing diatoms to dominate the phytoplankton community (Peperzak, et al. 1998).

The POC concentration was highest at the Coastal Station with 44.2 ± 1.3 μmol L^{-1}, 12.7 ± 1.6 μmol L^{-1} at the Oyster Ground and 17.8 ± 1.1 μmol L^{-1} at the Dogger Bank. The Chl *a* concentration was highest at the Coastal Station (3.1 ± 0.03 μg Chl *a* L^{-1}), lowest at the Oyster Ground (0.4 ± 0.04 μg Chl *a* L^{-1}) and increase again at the Dogger Bank (0.8 ± 0.03 μg Chl *a* L^{-1}). The other pigments showed the same pattern and are summarized in Table 2. Pigment composition and pigment ratios did not give clear indications about the dominating phytoplankton groups. The presence of fucoxanthin at all stations suggests the presence of diatoms, dinoflagellates, and haptophytes. Alongside fucoxanthin, haptophytes usually contain 19-butanoyloxyfocoxanthin and 19-hexanoyloxyfucoxanthin, both not detected in this study. However, the haptophyte *Phaeocystis globosa*, which is frequently encountered in the sampling area during May, can lack one or both (Schoemann et al. 2005). *P. globosa* was, therefore, considered a possible member of the phytoplankton community during the cruise.

Biochemical composition of POC

A total of 56% ± 1% to 82% ± 17% of total POC could be explained by carbohydrates, fatty acids, and amino acids (Fig. 5A). The main contributor to POC were the amino acids, which contributed 46% ± 11% (Coastal Station), 36% ± 8% (Dogger Bank), and 28% ± 4% (Oyster Ground). The second largest group contributing to POC were the neutral carbohydrates with 33% ± 6% (Coastal Station), 18% ± 5% (Oyster Ground), and 24% ± 6% (Dogger Bank). Fatty acids accounted for the lowest fraction of POC and contributed 3% ± 0.3% (Coastal Station), 2% ± 0.7% (Oyster Ground), and 5% ± 0.7% (Dogger Bank). All these values are in agreement with other publications that have investigated the biochemical composition of marine phytoplankton communities (Mock and Kroon 2002; Suárez and Marañón 2003).

A substantial amount of POC (18% ± 17% to 44% ± 1%) could not be identified. This unidentified fraction contains both DNA and RNA, and depending on resource availability these can contribute up to 30% of POC (Dortch et al. 1983). Other carbon compounds not quantified here include ATP, phytosterols, acidic sugars, and amino-sugars. Pigments contribute to total POC in a minor fraction as well. Furthermore, the effect of detrital carbon, either locally produced or derived from allochthonous inputs (especially at the Coastal Station), should be taken into account, which can possibly skew the carbon contribution to different macromolecules with respect to total living biomass. To access the current state of a phytoplankton community, it is, therefore, better to look at carbon fixation patterns instead of POC composition.

Carbon fixation rates within different macromolecule pools

Enrichment in $\delta^{13}C$ was detected in all bulk and macromolecule samples analyzed. Lowest $\Delta\delta^{13}C$ values ($\delta^{13}C_{sample} - \delta^{13}C_{background}$) were detected in the amino acid arginine at the Oyster Ground (35.7‰ ± 17.0‰, $n = 2$). Highest $\Delta\delta^{13}C$ reached 978.2‰ ± 25.1‰ ($n = 2$) for glucose, also at the Oyster Ground. Bulk $\Delta\delta^{13}C$ were moderate and ranged between 121.8‰ ± 31.6‰ ($n = 2$) and 261.4‰ ± 10.9‰ ($n = 2$).

The analytical error of the IRMS analysis is low. The method precision ranges between 0.2‰ (EA/IRMS) and 0.4‰ for certain individual compounds (LC/IRMS) (McCullagh et al. 2006; Boschker et al. 2008) and the aforementioned $\Delta\delta^{13}C$ imply that the final labeling concentration of 2% ^{13}C-DIC was sufficient to achieve $\Delta\delta^{13}C$ higher than the analytic error even for compounds that incorporate ^{13}C slowly (e.g., arginine). However, to achieve the precise detection of $\delta^{13}C$ values of individual compounds a minimum concentration of 36–150 ng carbon is required per compound in the sample volume injected onto the LC and GC columns (Boschker et al. 2008). We aimed for an average minimum concentration of 50 ng C per compound and sample injection. This required minimum concentration, the number of compounds that can be separated on the column of choice and the expected relative contribution of each macromolecule to total POC have to be considered during sampling to assure collection of sufficient material for extractions (see recommendations in Material and procedures section).

The standard deviations detected in this study were much higher than the analytical error and describe the experimental error, which derives from the natural variability in the community response to, for instance, small differences in incubation conditions of replicate carboys, for example, shading due to carboy position in incubator.

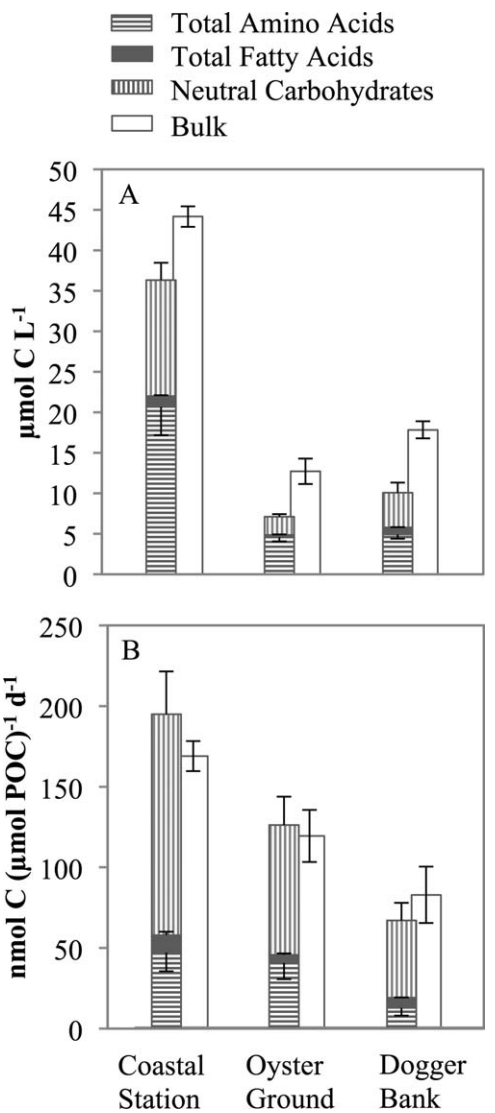

Fig. 5. Composition of POC (A) and biosynthesis rates of bulk carbon vs. biosynthesis rates of different macromolecule groups (B) for all three stations. The upper panel (A) expresses concentrations of POC and carbon within the different macromolecules in μmol C L^{-1}. Rates in panel (B) are in nmol C (μmol POC)$^{-1}$ d^{-1}. Shown are averages ± SD, $n = 2$.

Bulk carbon fixation rates after 24 h incubations were highest at the Coastal Station with 168.5 ± 9.3 nmol C (μmol POC)$^{-1}$ d^{-1} and declined to 119.0 ± 16.2 nmol C (μmol POC)$^{-1}$ d^{-1} and 82.4 ± 17.5 nmol C (μmol POC)$^{-1}$ d^{-1} at the Oyster Ground and Dogger Bank, respectively (Fig. 5B).

At all three stations, the highest relative amount of fixed carbon was allocated into neutral carbohydrates, followed by amino acids and fatty acids. At the Coastal Station, carbohydrates contributed a relative amount of 70% ± 0.4%, amino acids 24% ± 2%, and fatty acids 6% ± 2%. At the Dogger Bank, 64% ± 0.6% of carbon was allocated into carbohydrates, 32% ± 1% into amino acids and 4% ± 0.0% into fatty acids. Distribution at the Oyster Ground was 71% ± 10%, 19% ± 8%, and 9% ± 2% for carbohydrates, amino acids, and fatty acids, respectively (Fig. 5B).

Bulk vs. compound specific carbon fixation

The sum of carbon fixation within the different macromolecules is highest at the Coastal Station with 195.4 ± 39.8 nmol C (μmol POC^{-1}) d^{-1} and declines to 126.5 ± 29.1 nmol C (μmol POC^{-1}) d^{-1} and 67.4 ± 16.6 nmol C (μmol POC^{-1}) d^{-1} at the Oyster Ground and Dogger Bank, respectively (Fig. 5B). The sum of macromolecule carbon fixation was higher than the bulk carbon fixation at the Coastal Station and the Oyster Ground, accounting for 116% ± 29% and 104% ± 10%, respectively. At the Dogger Bank, the sum of biomolecule carbon fixation explained 82% ± 26% of bulk carbon fixation. Bulk carbon fixation was within the cumulative standard deviations of carbon fixation of macromolecule groups at all three stations, indicating no significant differences in the two approaches. Suárez and Marañón (2003) reported similar numbers in their study (95–104%) using a ^{14}C tracer approach. Overall, the compound specific approach is in agreement with the bulk approach and can also be used to describe the importance of one macromolecule group to bulk carbon fixation without investigating all macromolecule groups. Our results suggest that phytoplankton shuffle the majority of photosynthetically fixed carbon into the three macromolecule groups within 24 h, especially at the Coastal Station and the Oyster Ground, while phytoplankton at the Dogger Bank has at least one more important sink of carbon, potentially DNA and RNA.

Individual compounds

Carbohydrates

In terms of neutral carbohydrate composition, the Coastal Station and the Oyster Ground were almost identical. At both stations, glucose contributed 61% ± 10% and 64% ± 12% while Xyl/Man/Gal/Fru contributed 28% ± 6% and 28% ± 10% at both stations, and Ara/Fuc/Rib contributed 11% ± 2% and 8% ± 5%. At the Dogger Bank, glucose contributed only 53% ± 7% while Xyl/Man/Gal/Fru contributed 35% ± 10%, and Ara/Fuc/Rib 11% ± 6%. This resulted in ratios between glucose concentration to the other neutral carbohydrate of 1.6, 1.8, and 1.2 (Fig. 6A). Biosynthesis rates of the carbohydrate fractions deviated substantially from these concentration ratios at the Coastal Station and the Oyster Ground. There, glucose contributed 87% ± 14% to total synthesized carbohydrates, while Xyl/Man/Gal/Fru contributed 10% ± 3% and Ara/Fuc/Rib 3% ± 2% (numbers identical at both stations) resulting in ratios of 6.4 and 6.6. At the Dogger Bank, glucose contributed 66% ± 12%, Xyl/Man/Gal/Fru 28% ± 7%, and Ara/Fuc/Rib 6% ± 3%, a ratio of 1.9 (Fig. 6B). Possible explanations for such differences in ratios among stations can be threefold. First, the phytoplankton community at the Coastal Station and the Oyster Ground may have synthesized high amounts of internal storage polysaccharide, such as glucan or chysolaminaram (both made from glucose subunits), as a response to resource limitation causing increased detection of glucose synthesis. However, the approach shown here cannot distinguish between glucose derived from storage and nonstorage carbohydrates. Second, the phytoplankton community at the Dogger Bank used the glucose to either synthesize proteins and other macromolecules faster than at the other stations or excrete excessive amounts of carbohydrates. Third, the dominating phytoplankton species at the Coastal Station and the Oyster Ground possess additional external carbohydrates. Diatoms are known to produce carbohydrate-rich extracellular polymeric substances (Hoagland et al. 1993), and *Phaeocystis* spp., a haptophyte frequently encountered in the study area, forms a colony matrix rich in mucosaccharides (Alderkamp et al. 2006). External carbohydrates from both phytoplankton groups would be extracted with the intracellular neutral carbohydrates using the described method. Overall, high concentrations of carbohydrates reduce the nutritional value of the phytoplankton for higher trophic levels. However, high amounts of extracellular carbohydrates can also fuel heterotrophic activity by bacteria (Borsheim et al. 2005; Alderkamp et al. 2007).

Amino acids

At all three stations, the three most abundant amino acids comprised over 40% of the total amino acid concentration (Fig. 6C). At the Coastal Station and the Oyster Ground, leucine (Leu) was the most important amino acids, followed by proline (Pro) and threonine (Thr). At the Dogger Bank, glutamic acid + glutamine (Glu) showed highest abundances followed by Leu and Thr (Fig. 6C). Other important amino acids at all three stations were lysine (Lys), phenylalanine (Phe), and valine (Val), however, they had different relative concentrations at the investigated stations. The above listed amino acids also showed highest biosynthesis rates with an identical distribution pattern (Fig. 6D).

Within the amino acid pool, an indicator for N-limitation is the accumulation of Glu in the cells and a consequent reduction of Pro. Proline is directly synthesized from glutamate and this synthesis is dependent on nitrogen

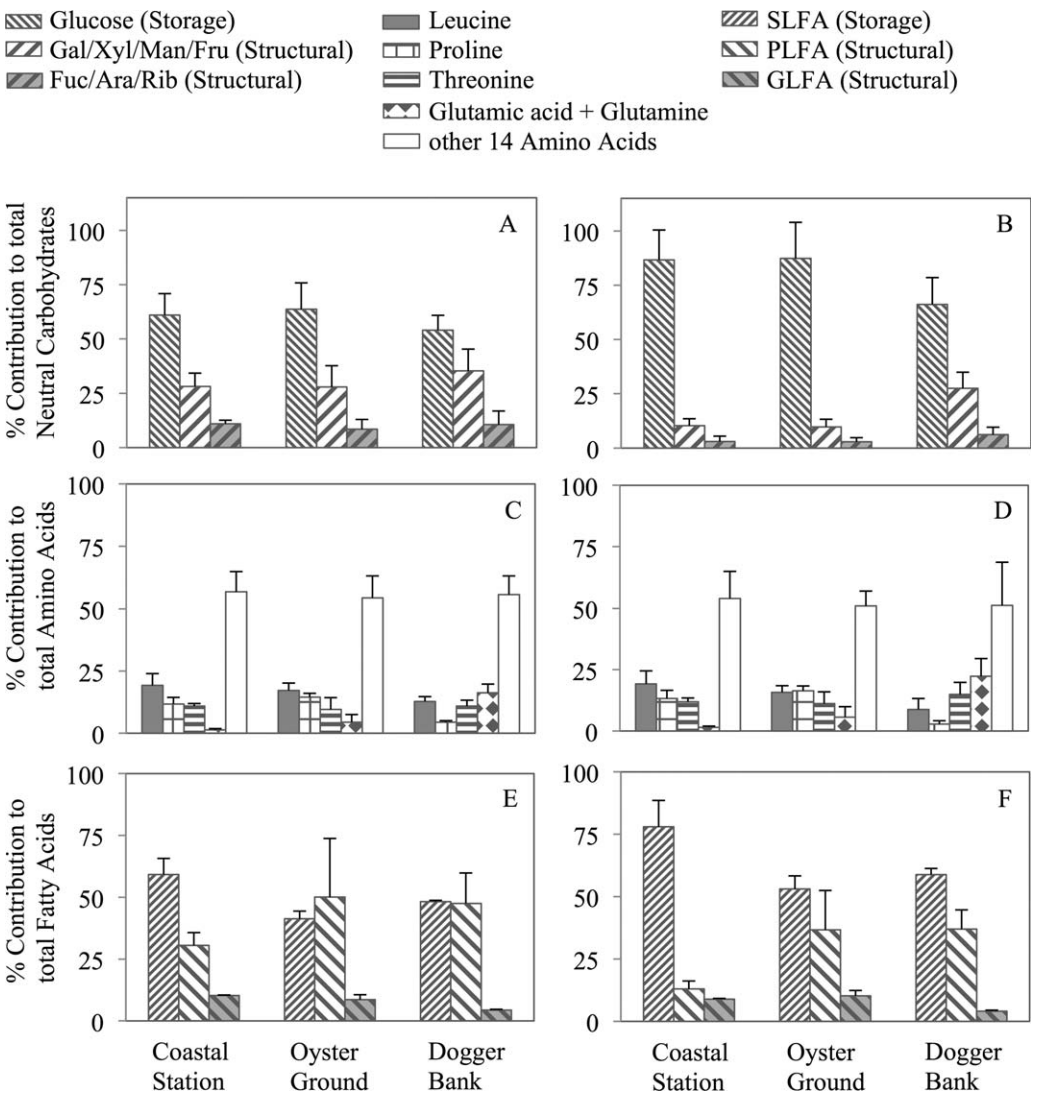

Fig. 6. Contribution of individual compounds within the different macromolecule groups. Total neutral carbohydrate composition (A) and biosynthesis (B) was divided into glucose, co-elution of galactose/xylose/mannose/fructose (Gal/Xyl/Man/Fru) and co-elution of fucose/arabinose/ribose (Fuc/Ara/Rib). Total amino acid concentrations (C) and biosynthesis (D) show the three most important amino acids, and additionally Glu (Coastal Station and Oyster Ground) or Pro (Dogger Bank). The "other 14 amino acids" are the sum of remaining 14 of all 18 amino acids measured per station. Total fatty acid concentrations (E) and biosynthesis (F) were divided into storage lipids (SLFA) and structural lipids, which were further divided into glycolipids (GLFA) and phospholipids (PLFA). Shown are averages ± SD, $n = 2$.

assimilation into the cell, which can be affected by nitrogen availability in the environment or ultraviolet-B radiation (Goes et al. 1995). The ratio of Pro: Glu could, therefore, potentially be used to identify N-limited phytoplankton communities. The distribution of the main amino acids on the Coastal Station and the Oyster Ground was very similar, with Pro being one of the most abundant amino acids. At the Coastal Station, Pro: Glu ratios for concentrations and biosynthesis rates were 10.1 ± 6.1 and 9.7 ± 5.3, respectively, suggesting that Glu could be rapidly synthesized into Pro and N-availability was not limiting. At the Oyster Ground, Pro: Glu ratios decreased to 4.2 ± 2.6 and 3.9 ± 2.6, for concentrations and biosynthesis rates, respectively, suggesting a slower conversion. At the Doggers Bank in contrast, the ongoing low availability of nitrogen led to an accumulation of Glu in the cells, while Pro was of very low importance which resulted in very low Pro: Glu ratios of 0.3 ± 0.01 for concentrations and 0.1 ± 0.02 for biosynthesis rates.

The amino acids Leu, Val, Thr, Phe, and Lys, are all essential amino acids and cannot be synthesized by higher trophic levels, hence must be taken up through the diet. Together with the other essential amino acids measured (Arg, His, Ile, Met) they contributed 69% ± 1%, 64% ± 1%, and 57% ± 1% of total amino acids at the Coastal Station, Oyster Ground,

Table 3. Fatty acid concentrations found in the PLFA fraction at each station. Concentrations are given in nmol C (μmol POC)$^{-1}$. nd, not detected. Averages ± SD are shown ($n = 2$).

	Coastal Station	Oyster Ground	Dogger Bank
14:0	0.82±0.13	0.58±0.39	2.56±0.51
16:0	0.95±0.12	2.12±1.05	3.08±0.77
18:0	0.47±0.22	0.46±0.14	0.39±0.09
16:1ω7c	0.77±0.14	1.97±1.00	4.18±0.84
18:1ω9c	0.18±0.06	0.32±0.14	0.64±0.13
18:1ω7c	0.59±0.16	1.08±0.41	0.84±0.27
16:2ω4	0.05±0.06	0.05±0.02	0.28±0.04
16:3ω3	0.09±0.05	0.08±0.02	0.09±0.02
16:3ω4	nd	nd	nd
16:4ω1	nd	nd	nd
18:2ω6c	0.14±0.10	0.38±0.13	0.35±0.06
18:3ω3	0.13±0.05	0.27±0.11	0.50±0.09
18:4ω3	0.26±0.09	0.83±0.41	0.90±0.18
18:5ω3	0.07±0.04	0.22±0.10	0.52±0.41
18:5ω5	0.10±0.02	0.24±0.11	0.72±0.02
20:5ω3	1.85±0.68	1.39±0.69	3.82±1.16
22:6ω3	1.86±0.54	2.20±1.05	6.45±2.10

and Dogger Bank, respectively. From an amino acid perspective, the phytoplankton at the Coastal Station had the highest nutritional value for higher trophic levels while N-limitation may reduce the nutritional value at the Dogger Bank.

Fatty acids

Fatty acids were least abundant in the GLFA fraction, which contributed $4\% \pm 0.3\% - 10\% \pm 0.2\%$ of total fatty acids in both concentration and biosynthesis (Fig. 6E,F). A recent study by Heinzelmann et al. (2014) shows that the separation of glycolipids from phospholipids by commonly used silicate column chromatography is incomplete, and that glyco- and other lipids also elute in the methanol fraction. However, both glyco- and phospholipids are structural (membrane) lipids in contrast to the neutral storage lipids in the chloroform fraction, and therefore, the data for these two membrane fractions was combined in this study.

There was considerable variation in the fatty acid composition between stations. Phytoplankton from the Coastal Station contained more storage lipids than structural lipids (ratio 1.5 ± 0.01), whereas phytoplankton at the Oyster Ground and the Dogger Bank contained similar concentrations of storage lipids and structural lipids with ratios of 0.7 ± 0.3 and 0.9 ± 0.2, respectively (Fig. 6E). A similar order was found in the biosynthesis of fatty acids. However, the contribution of storage lipids was increased at all three stations, which resulted in ratios of 3.6 ± 0.1, 1.1 ± 0.3, and 1.4 ± 0.4, respectively. An accumulation of storage fatty acids compared with structural fatty acids can be used as indicator for resource limitation (N or P). In this study, it indicates a nutrient limitation at the Coastal Station compared with the other two stations.

The composition of individual fatty acids in the PLFA fraction can be used to identify the dominating phytoplankton groups within a community. Diatoms are enriched in 16:1ω7 and 20:5ω3, and contain the biomarker PLFAs 16:3ω4 and 16:4ω1, while dinoflagellates and haptohytes show increased concentrations in 18:4ω3 and 22:6ω3, and have the biomarker PLFAs 18:5ω3 and 18:5ω5 (Dijkman and Kromkamp 2006). The lack of diatom biomarkers 16:3ω4 and 16:4ω1 at all three stations confirm that diatoms were not major part of the phytoplankton community. The presence of PUFAs with 18 carbons indicates that dinoflagellates and haptophytes (including *P. globosa*) were dominating the phytoplankton community (Table 3). The low availability of inorganic N and P as well as the lack of $Si(OH)_4$ support that conditions were unfavorable for diatoms, while more favorable for dinoflagellates and haptophytes, which do not rely on $Si(OH)_4$ and are known to be capable of accessing the organic P pool (Schoemann et al. 2005; Dyhrman and Ruttenberg 2006).

Overall, the increased synthesis of carbohydrate and fatty acid storage products indicates that conditions for phytoplankton were not optimal. The P-limitation at the Coastal Station had a direct effect on PLFA synthesis while the N-limitation at the Dogger Bank directly affected amino acids synthesis. Under these suboptimal conditions, the increased synthesis of storage products did not require N or P. Additionally, there might have been indirect effects, as P is also required for ATP and N is required for gene-expression/rRNA synthesis as well as for enzymes to catalyze reactions within the cell. Furthermore, the lack of $Si(OH)_4$ affects diatom growth in a negative way.

Discussion

The presented approach is a combination of established and new CSIA methods (Fig. 1). All methods utilize stable carbon isotopes as tracer (^{13}C) instead of radioactive ^{14}C isotopes. Several advantages make ^{13}C the isotope of choice. No special regulations and permissions have to be followed and obtained working with stable isotopes. However, the ^{13}C method is less sensitive and relatively large volumes are required for incubations to obtain enough biomass for extractions (between $\sim$ 70 μg and 600 μg of POC, depending on the macromolecules of interest). So far, studies using a ^{14}C approach to identify carbon-fixation into macromolecules only investigated different groups of macromolecules but not individual compounds within those groups (Marañón et al. 1995; Suárez and Marañón 2003). Separation of the building blocks of these macromolecule groups is possible on LC- and GC-columns and the individual compounds are directly introduced into the IRMS instrument, increasing the detail of information. LC- separation is preferred over

GC-separation because derivatization and correction thereof is not necessary at an even higher analytical precision (McCullagh et al. 2006). Furthermore, the use of LC/or GC/C-IRMS is preferred over the use of LC- or GC–MS systems because the IRMS systems are far more sensitive in terms of ^{13}C labeling. The mass spectrometer system requires the addition of high amounts of ^{13}C label to the incubation (> 15% ^{13}C) for an accurate calculation of compound specific uptake rates (Hama and Handa 1992). In our approach, ^{13}C enrichment can be kept at 2% ^{13}C or less to achieve well detectable changes in $\Delta\delta^{13}C$ values.

The combination of these methods is labor intensive but the obtained results provide a highly detailed view into the fate of carbon fixed through photosynthesis. Although the presented dataset is small, we identified P-limitation and N-limitation at the different stations based on the prevailing N:P nutrient ratios. Culture-based studies show that a lack of N or P results in a build-up in storage carbohydrates and storage lipids (Granum et al. 2002; Borsheim et al. 2005). Differences in nutrient N:P ratios do not seem to affect the relative POC composition with respect to the different macromolecule (sub-) groups, hence cannot be used to deduce prevailing resource limitation. However, differences in carbon fixation patterns can give insight as seen in our field data. At all three stations carbon fixation into glucose is high, which could indicate increased biosynthesis of the storage products glucan and chrysolaminarin. SLFAs contribute more than 50% of total fatty acids also implying resource limitation. Amino acids synthesis seems to be most affected by the availability of nitrogen, as previously shown by Tapia et al. (1996). A good indicator for N-limitation might be a low Pro: Glu ratio, caused by the accumulation of Glu, which cannot be further synthesized into Pro when N-availability in the environment is limited (Goes et al. 1995). At the Dogger Bank, low Pro: Glu ratios in concentrations and biosynthesis rates support assumption that N-limitation was prevailing which is in accordance with the low N:P ratio. However, additional experiments are necessary to identify the limiting nutrient and its specific consequences for the synthesis of different macromolecule groups or individual compounds. For example, nutrient addition experiments in the field could support studies like the one presented here and culture-based studies could describe species-specific adaptations to nutrient limitations. The approach may be used to prove model predictions on the effects of nutrient limitations (Klausmeier et al. 2004) directly in the field and improve our understanding of differences in stoichiometric composition of phytoplankton (Geider and LaRoche 2002), to obtain information on physiological states of phytoplankton, and to evaluate its quality as food for higher trophic levels (Sterner et al. 1993; Plath and Boersma 2001). The incubation time for nutrient addition experiments can be kept short ($\leq$ 24 h) and changes in community composition, which can occur in classical bioassays with much longer incubation periods (Beardall et al. 2001), are avoided and guarantee field relevant results. Compounds specific labeling with stable isotopes can also be used to identify synthesis pathways of individual compounds or investigate physiological responses to different light levels, growth rates, or nutrient sources. All or selected methods can be applied to study effects of viral infection or trace consumption of phytoplankton through the food web.

Our study was performed in a temperate coastal sea with moderate to high phytoplankton densities and we used filtration volumes between 1.0 L and 2.0 L to obtain sufficient material for macromolecule extractions. As long as adequate amounts of biomass are collected for extraction (e.g., by adapting the filtration volume), the presented suite of methods can be applied to other ecosystems such as estuaries, the oligotrophic ocean, but also to sediments and consumer organisms (e.g., zooplankton). The described methods are quite versatile and can be adapted to specific research questions. For example, we obtained a high resolution in our fatty acids by separating samples into subfractions to obtain data for storage and structural fatty acids. However, if this high resolution is not necessary, the total lipid extract can already be derivatized and analyzed without a preceding separation on a silicate column. Although that decreases the detail of information it also reduces the number of samples and hence the runtime of the machine as well as data analysis. The same is applicable for the analysis of carbohydrates. We choose a column that only separates glucose, while the other carbohydrates co-elute in two peaks. Alternatively, the Carbopac PA20 column (Thermo Fisher Scientific) can be used to furthermore separate the co-eluting carbohydrates (Boschker et al. 2008). However, we observed that during hydrolysis of the samples a yet unknown component leaches from the filter (most likely silicate). The clean-up step described in the method section removes the majority of this compound. However, the low amount of carbohydrates in our samples required a large sample volume to be injected into the column, which only slowly eluted from the column, and made it necessary to regenerate the Carbopac PA20 column after each run. This is highly time consuming when handling a large number of samples, and we therefore, decided to use the Aminex HPX-87H column as an alternative as it is highly insensitive to salts at the cost of a lower separation power.

Overall, uptake studies with ^{13}C-enriched compounds are ideal to investigate in situ processes (Boschker and Middelburg 2002). Incubation periods of a few hours to a day (24 h) make possible changes in community composition and activity negligible. Furthermore, possible effects of for example, allochthonous detritus (as at our Coastal Station) are minimized as only biosynthesis rates are considered.

Recently, Moerdijk-Poortvliet et al. (2014) developed a method to measure DNA and RNA nucleotide concentrations and $\delta^{13}C$ values by LC/IRMS. Adding their method to our approach makes it possible to assemble a carbon budget

including all four major macromolecules that make up the majority of phytoplankton biomass. The range of labeled compounds present in phytoplankton is vast, so is the still growing number of compounds that can be analyzed by LC/ and GC/C-IRMS. Combining CSIA with other tools, such as the identification of active organisms by molecular methods, will help to increase our knowledge of important carbon cycle processes, their drivers, and consequences for the ecosystem.

References

Abaye, D. A., D. J. Morrison, and T. Preston. 2011. Strong anion exchange liquid chromatographic separation of protein amino acids for natural ^{13}C-abundance determination by isotope ratio mass spectrometry. Rapid Commun. Mass Spectrom. **25**: 429–435. doi:10.1002/rcm.4844

Alderkamp, A.-C., A. G. J. Buma, and M. van Rijssel. 2007. The carbohydrates of *Phaeocystis* and their degradation in the microbial food web. Biogeochemistry **83**: 99–118. doi:10.1007/s10533-007-9078-2

Alderkamp, A. C., J. C. Nejstgaard, P. G. Verity, M. J. Zirbel, A. F. Sazhin, and M. van Rijssel. 2006. Dynamics in carbohydrate composition of *Phaeocystis pouchetii* colonies during spring blooms in mesocosms. J. Sea Res. **55**: 169–181. doi:10.1016/j.seares.2005.10.005

Beardall, J., E. Young, and S. Roberts. 2001. Approaches for determining phytoplankton nutrient limitation. Aquat. Sci. **63**: 44–69. doi:10.1007/PL00001344

Bligh, E. G., and W. J. Dyer. 1959. A rapid method of total lipid extraction and purification. Can. J. Biochem. Physiol. **37**: 911–917. doi:10.1139/o59-099

Borsheim, K. Y., O. Vadstein, S. M. Myklestad, H. Reinertsen, S. Kirkvold, and Y. Olsen. 2005. Photosynthetic algal production, accumulation and release of phytoplankton storage carbohydrates and bacterial production in a gradient in daily nutrient supply. J. Plankton Res. **27**: 743–755. doi:10.1093/plankt/fbi047

Boschker, H. T. S. 2004. Linking microbial community structure and functioning: Stable isotope (^{13}C) labeling in combination with PLFA analysis, p. 1673–1688. *In* G. A. Kowalchuk, F.J. de Bruijn, I.M. Head, A.D.Akkermans and J.D. van Elsas [eds.], Molecular microbial ecology manual II. Kluwer Academic.

Boschker, H. T. S., E. M. J. Dekkers, R. Pel, and T. E. Cappenberg. 1995. Sources of organic-carbonin the littoral of Lake Gloomier as indicated by stable carbon-isotope and carbohydrates compositions. Biogeochemistry **29**: 89–105. doi:10.1007/BF00002596

Boschker, H. T. S., and J. J. Middelburg. 2002. Stable isotopes and biomarkers in microbial ecology. FEMS Microbiol. Ecol. **40**: 85–95. doi:10.1111/j.1574-6941.2002.tb00940.x

Boschker, H. T. S., T. C. W. Moerdijk-Poortvliet, P. van Breugel, M. Houtekamer, and J. J. Middelburg. 2008. A versatile method for stable carbon isotope analysis of carbohydrates by high-performance liquid chromatography/ isotope ratio mass spectrometry. Rapid Commun. Mass Spectrom. **22**: 3902–3908. doi:10.1002/rcm.3804

Carpenter, E. J., A. Subramaniam, and D. G. Capone. 2004. Biomass and primary productivity of the cyanobacterium *Trichodesmium* spp. in the tropical N Atlantic ocean. Deep Sea Res. Part I. **51**: 173–203. doi:10.1016/j.dsr.2003.10.006

Charpin, M. F., N. Maurin, C. Amblard, and J. Devaux. 1998. Seasonal variations of phytoplankton photosynthate partitioning in two lakes of different trophic level. J. Plankton Res. **20**: 901–921. doi:10.1093/plankt/20.5.901

Cullen, J. J. 2001. Primary Production Methods, p. 578–584. In John H. Steele [ed.], Encyclopedia of Ocean Sciences (Second Edition), Academic Press, Oxford.

Degerholm, J., K. Gundersen, B. Bergman, and E. Soderback. 2006. Phosphorus-limited growth dynamics in two Baltic Sea cyanobacteria, *Nodularia* sp and *Aphanizomenon* sp. FEMS Microbiol. Ecol. **58**: 323–332. doi:10.1111/j.1574-6941.2006.00180.x

Dijkman, N. A., H. T. S. Boschker, L. J. Stal, and J. C. Kromkamp. 2010. Composition and heterogeneity of the microbial community in a coastal microbial mat as revealed by the analysis of pigments and phospholipid-derived fatty acids. J. Sea Res. **63**: 62–70. doi:10.1016/j.seares.2009.10.002

Dijkman, N. A., and J. C. Kromkamp. 2006. Phospholipid-derived fatty acids as chemotaxonomic markers for phytoplankton: Application for inferring phytoplankton composition. Mar. Ecol. Prog. Ser. **324**: 113–125. doi:10.3354/meps324113

Dortch, Q., T. L. Roberts, J. R. Clayton, and S. I. Ahmed. 1983. RNA DNA ratios and DNA concentrations as indicators of growth-rate and biomass in planktonic marine organisms. Mar. Ecol. Prog. Ser. **13**: 61–71. doi:10.3354/meps013061

Dyhrman, S. T., and K. C. Ruttenberg. 2006. Presence and regulation of alkaline phosphatase activity in eukaryotic phytoplankton from the coastal ocean: Implications for dissolved organic phosphorus remineralization. Limnol. Oceanogr. **51**: 1381–1390. doi:10.4319/lo.2006.51.3.1381

Falkowski, P. G. 2000. Rationalizing elemental ratios in unicellular algae. J. Phycol. **36**: 3–6. doi:10.1046/j.1529-8817.2000.99161.x

Field, C. B., M. J. Behrenfeld, J. T. Randerson, and P. Falkowski. 1998. Primary production of the biosphere: Integrating terrestrial and oceanic components. Science **281**: 237–240. doi:10.1126/science.281.5374.237

Gallon, J. R., and others. 2002. Maximum rates of N_2 fixation and primary production are out of phase in a developing cyanobacterial bloom in the Baltic Sea. Limnol. Oceanogr. **47**: 1514–1521. doi:10.4319/lo.2002.47.5.1514

Geider, R. J., and J. LaRoche. 2002. Redfield revisited: Variability of C:N:P in marine microalgae and its biochemical

basis. Eur. J. Phycol. **37**: 1–17. doi:10.1017/S0967026201003456

Godin, J.-P., L.-B. Fay, and G. Hopfgartner. 2007. Liquid chromatography combined with mass spectrometry for ^{13}C isotopic analysis in life science research. Mass Spectrom. Rev. **26**: 751–774. doi:10.1002/mas.20149

Goes, J. I., N. Handa, S. Taguchi, and T. Hama. 1995. Changes in the patterns of biosynthesis and composition of amino acids in a marine phytoplankter exposed to ultraviolet-B radiation: Nitrogen limitation implicated. Photochem. Photobiol. **62**: 703–710. doi:10.1111/j.1751-1097.1995.tb08719.x

Gosselin, M., M. Levasseur, P. A. Wheeler, R. A. Horner, and B. C. Booth. 1997. New measurements of phytoplankton and ice algal production in the Arctic Ocean. Deep Sea Res. Part II. **44**: 1623–1644. doi:10.1016/s0967-0645(97)00054-4

Granum, E., S. Kirkvold, and S. M. Myklestad. 2002. Cellular and extracellular production of carbohydrates and amino acids by the marine diatom *Skeletonema costatum*: Diel variations and effects of N depletion. Mar. Ecol. Prog. Ser. **242**: 83–94. doi:10.3354/meps242083

Hama, J., and N. Handa. 1992. Diel photosynthetic production of cellular organic-matter in natural phytoplankton populations, measured with ^{13}C and gas-chromatography mass-spectrometry. 1. Monosaccharides. Mar. Biol. **112**: 175–181. doi:10.1007/BF00702459

Heinzelmann, S. M., N. J. Bale, E. C. Hopmans, J. S. S. Damste, S. Schouten, and M. T. J. van der Meer. 2014. Critical assessment of glyco- and phospholipid separation by using silica chromatography. Appl. Environ. Microbiol. **80**: 360–365. doi:10.1128/aem.02817-13

Hoagland, K. D., J. R. Rosowski, M. R. Gretz, and S. C. Roemer. 1993. Diatom extracellular polymeric substances—function, fine-structure, chemistry, and physiology. J. Phycol. **29**: 537–566. doi:10.1111/j.0022-3646.1993.00537.x

Karl, D. M., J. R. Christian, J. E. Dore, D. V. Hebel, R. M. Letelier, L. M. Tupas, and C. D. Winn. 1996. Seasonal and interannual variability in primary production and particle flux at Station ALOHA. Deep Sea Res. Part II. **43**: 539–568. doi:10.1016/0967-0645(96)00002-1

Klausmeier, C. A., E. Litchman, T. Daufresne, and S. A. Levin. 2004. Optimal nitrogen-to-phosphorus stoichiometry of phytoplankton. Nature **429**: 171–174. doi:10.1038/nature02454

Krummen, M., A. W. Hilkert, D. Juchelka, A. Duhr, H. J. Schluter, and R. Pesch. 2004. A new concept for isotope ratio monitoring liquid chromatography/mass spectrometry. Rapid Commun. Mass Spectrom. **18**: 2260–2266. doi:10.1002/rcm.1620

Marañón, E., E. Fernandez, and R. Anadon. 1995. Patterns of macromolecular-synthesis by natural phytoplankton assemblages under changing upwelling regimes—in-situ observations and microcosm experiments. J. Exp. Mar. Biol. Ecol. **188**: 1–28. doi:10.1016/0022-0981(94)00177-F

McCarthy, M. D., J. Lehman, and R. Kudela. 2013. Compound-specific amino acid $\delta^{15}N$ patterns in marine algae: Tracer potential for cyanobacterial vs. eukaryotic organic nitrogen sources in the ocean. Geochim. Cosmochim. Acta **103**: 104–120. doi:10.1016/j.gca.2012.10.037

McCullagh, J., J. Gaye-Siessegger, and U. Focken. 2008. Determination of underivatized amino acid $\delta^{13}C$ by liquid chromatography/isotope ratio mass spectrometry for nutritional studies: The effect of dietary non-essential amino acid profile on the isotopic signature of individual amino acids in fish. Rapid Commun. Mass Spectrom. **22**: 1817–1822. doi:10.1002/rcm.3554

McCullagh, J. S. O., D. Juchelka, and R. E. M. Hedges. 2006. Analysis of amino acid ^{13}C abundance from human and faunal bone collagen using liquid chromatography/isotope ratio mass spectrometry. Rapid Commun. Mass Spectrom. **20**: 2761–2768. doi:10.1002/rcm.2651

Middelburg, J. J., C. Barranguet, H. T. S. Boschker, P. M. J. Herman, T. Moens, and C. H. R. Heip. 2000. The fate of intertidal microphytobenthos carbon: An in situ ^{13}C labeling study. Limnol. Oceanogr. **45**: 1224–1234. doi:10.4319/lo.2000.45.6.1224

Miyatake, T., T. C. W. Moerdijk-Poortvliet, L. J. Stal, and H. T. S. Boschker. 2014. Tracing carbon flow from microphytobenthos to major bacterial groups in an intertidal marine sediment by using an in situ ^{13}C pulse-chase method. Limnol. Oceanogr. **59**: 1275–1287. doi:10.4319/lo.2014.59.4.1275

Mock, T., and B. M. A. Kroon. 2002. Photosynthetic energy conversion under extreme conditions—I: Important role of lipids as structural modulators and energy sink under N-limited growth in Antarctic sea ice diatoms. Phytochemistry **61**: 41–51. doi:10.1016/S0031-9422(02)00216-9

Moerdijk-Poortvliet, T. C. W., J. Brasser, G. de Ruiter, M. Houtekamer, H. Bolhuis, L. J. Stal, and H. T. S. Boschker. 2014. A versatile method for simultaneous stable carbon isotope analysis of DNA and RNA nucleotides by liquid chromatography/isotope ratio mass spectrometry. Rapid Commun. Mass Spectrom. **28**: 1401–1411. doi:10.1002/rcm.6919

Montoya, J. P., M. Voss, P. Kähler, and D. G. Capone. 1996. A simple, high-precision, high-sensitive tracer assay for N_2 fixation. Appl. Environ. Microbiol. **62**: 986–993.

Moodley, L., J. Middelburg, K. Soetaert, H. T. S. Boschker, P. M. J. Herman, and C. Heip. 2005. Similar rapid response to phytodetritus deposition in shallow and deep-sea sediments. J. Mar. Res. **63**: 457–469. doi:10.1357/0022240053693662

Oakes, J. M., B. D. Eyre, J. J. Middelburg, and H. T. S. Boschker. 2010. Composition, production, and loss of carbohydrates in subtropical shallow subtidal sandy sediments: Rapid processing and long-term retention revealed by ^{13}C-labeling. Limnol. Oceanogr. **55**: 2126–2138. doi:10.4319/lo.2010.55.5.2126

Peperzak, L., F. Colijn, W. W. C. Gieskes, and J. C. H. Peeters. 1998. Development of the diatom-*Phaeocystis* spring bloom in the Dutch coastal zone of the North Sea: The silicon depletion versus the daily irradiance threshold hypothesis. J. Plankton Res. **20**: 517–537. doi:10.1093/plankt/20.3.517

Plath, K., and M. Boersma. 2001. Mineral limitation of zooplankton: Stoichiometric constraints and optimal foraging. Ecology **82**: 1260–1269. doi:10.1890/0012-9658(2001)082[1260:mlozsc]2.0.co;2

Rieley, G. 1994. Derivatization of organic-compounds prior to gas-chromatographic combustion-isotope ratio mass spectrometric analysis—identification of isotope fractionation processes. Analyst **119**: 915–919. doi:10.1039/an9941900915

Rijstenbil, J. W. 2003. Effects of UVB radiation and salt stress on growth, pigments and antioxidative defence of the marine diatom *Cylindrotheca closterium*. Mar. Ecol. Prog. Ser. **254**: 37–48. doi:10.3354/meps254037

Schoemann, V., S. Becquevort, J. Stefels, W. Rousseau, and C. Lancelot. 2005. Phaeocystis blooms in the global ocean and their controlling mechanisms: A review. J. Sea Res. **53**: 43–66. doi:10.1016/j.seares.2004.01.008

Shiozaki, T., K. Furuya, T. Kodama, S. Kitajima, S. Takeda, T. Takemura, and J. Kanda. 2010. New estimation of N_2 fixation in the western and central Pacific Ocean and its marginal seas. Global Biogeochem. Cycles **24**. doi:10.1029/2009gb003620

Steeman-Nielsen, E. 1952. The use of radioactive carbon (^{14}C) for measuring organic production in the sea. J. Cons. **18**: 117–140. doi:10.1093/icesjms/18.2.117

Sterner, R. W., D. D. Hagemeier, and W. L. Smith. 1993. Phytoplankton nutrient limitation and food quality in Daphnia. Limnol. Oceanogr. **38**: 857–871. doi:10.4319/lo.1993.38.4.0857

Suárez, I., and E. Marañón. 2003. Photosynthate allocation in a temperate sea over an annual cycle: The relationship between protein synthesis and phytoplankton physiological state. J. Sea Res. **50**: 285–299. doi:10.1016/j.seares.2003.04.002

Tapia, M., J. deAlda, M. Llama, and J. Serra. 1996. Changes in intracellular amino acid and organic acids induced by nitrogen starvation and nitrate or ammonium resupply in the cyanobacterium *Phormidium laminosum*. Planta **198**: 526–531. doi:10.1007/BF00262638

Van Den Meersche, K., J. J. Middelburg, K. Soetaert, P. Van Rijswijk, H. T. S. Boschker, and C. H. R. Heip. 2004. Carbon-nitrogen coupling and algal-bacterial interactions during an experimental bloom: Modeling a ^{13}C tracer experiment. Limnol. Oceanogr. **49**: 862–878. doi:10.4319/lo.2004.49.3.0862

Veuger, B., B. D. Eyre, D. Maher, and J. J. Middelburg. 2007. Nitrogen incorporation and retention by bacteria, algae, and fauna in a subtropical intertidal sediment: An in situ ^{15}N labeling study. Limnol. Oceanogr. **52**: 1930–1942. doi:10.4319/lo.2007.52.5.1930

Veuger, B., J. J. Middelburg, H. T. S. Boschker, and M. Houtekamer. 2005. Analysis of ^{15}N incorporation into D-alanine: A new method for tracing nitrogen uptake by bacteria. Limnol. Oceanogr. Methods. **3**: 230–240. doi:10.4319/lom.2005.3.230

Wannicke, N., B. P. Koch, and M. Voss. 2009. Release of fixed N_2 and C as dissolved compounds by *Trichodesmium erythreum* and *Nodularia spumigena* under the influence of high light and high nutrient (P). Aquat. Microb. Ecol. **57**: 175–189. doi:10.3354/ame01343

Acknowledgments

Special thanks to the crew from the R/V Pelagia for their help and support during the cruise. The authors also thank the Nutrient Lab at NIOZ-Texel for providing nutrient data, the Analytical Lab at NIOZ-Yerseke for the analysis of pigment samples and the editor and two anonymous reviewers for constructive feedback. This research was supported by the Netherlands Organization for Scientific Research (NWO) to HTSB (grant ZKO 839.10.511).

Submitted 22 August 2014
Revised 4 March 2015
Accepted 5 March 2015

Associate editor: Prof. Claudia Benitez-Nelson